Angle-Scanning Photonic Crystal Enhanced Fluorescence Microscopy

Vikram Chaudhery, Meng Lu, Anusha Pokhriyal, Stephen C. Schulz, and Brian T. Cunningham, *Senior Member, IEEE*

***Abstract*—Photonic crystal enhanced fluorescence (PCEF) has been demonstrated as an effective means for amplifying the excitation provided to surface-bound fluorescent molecules while simultaneously enhancing fluorescence emission collection efficiency. Optimal coupling of a fluorophore-exciting light source to the PC occurs with the use of collimated plane waves, as utilized in a special-purpose fluorescence microscope specifically designed for coupling with PCEF surfaces. However, PCEF surfaces are also capable of coupling light from focused sources, such as those used in commercially available confocal laser scanners, but with a reduction in the obtainable enhancement factor. Using computer simulations and experimental measurements, we describe the interaction between the resonant bandwidth of a PCEF device surface and the optical design of the detection instrumentation that is used to provide fluorescence excitation. We show that highly collimated illumination is required for achieving the greatest PCEF enhancement factors, but at the expense of poor tolerance to nonuniformities in resonant wavelength across the PCEF surface. To overcome this limitation, we demonstrate a fixed wavelength/multiple incident angle scanning detection system that is capable of measuring every pixel in a PCEF fluorescence image under conditions that optimize resonant excitation efficiency.**

***Index Terms*—Fluorescence, microscopy, photonic crystals.**

I. Introduction

FLOURESCENCE has emerged as a useful tool for imaging and detection in medical and biological sciences due to its excellent sensitivity, wide availability of dye molecules, ease of application to broad classes of biomolecules, and robust detection instrumentation. The major limitation of fluorescence is the strength of signals that can often limit visualization and quantification of low concentration analytes in numerous fluorescence based assays [1], [2]. To address the need for higher sensitivity and improved signal-to-noise ratios (SNR) in surface-based fluorescence assays, dielectric-based photonic crystal (PC) surfaces have been utilized in the context of gene expression analysis [3], protein biomarker detection [4].

PC surfaces provide a consistent and highly efficient platform for enhancement of fluorescence by exploiting their optical resonance characteristics to provide a heightened excitation field (resulting in a phenomenon called "enhanced excitation") along with the ability to control the photonic dispersion which provides a powerful mechanism to redirect the emitted light into certain preferred directions, where it can be detected with greater efficiency ("enhanced extraction"). The simultaneous implementation of these two techniques has been shown to boost the radiation detected from quantum dots and fluorescent dye molecules by two orders of magnitude [5]–[8].

While the effects of PC enhanced excitation and enhanced extraction can be combined with multiplicative effects [7]–[9] this work is primarily concerned with optimization of enhanced excitation through the interaction of the PC resonant mode characteristics and the degree of collimation of the illumination that is provided to the PC. The enhanced excitation and extraction mechanisms have been shown not to alter the fluorophore lifetime by the Purcell effect [6] when a PC with moderate Q-factor (Q is mathematically defined as $\lambda/\Delta\lambda$, where λ is the resonant wavelength, and $\Delta\lambda$ is the full-width at half maximum of the resonant peak spectrum) is used.

In our previous work, a confocal laser scanner, incorporating a focused laser beam, was used to good effect for PCEF [9], [10]. However, due to the angle selectivity of the PCEF surface, only a portion of the excitation energy can be coupled into the resonance mode and contribute to enhanced fluorescence emission. To improve PCEF performance, we demonstrated the use of a collimated excitation scheme [7], in which the excitation beam matches the resonance angle of the target resonance mode. In the detection instrument described in our previous work, a single excitation angle (at a fixed illumination wavelength) was selected for imaging an entire PC surface. Using this fixed angle/fixed wavelength excitation approach, only limited regions of a high-Q PCEF surface could be optimally excited. While some parts of the PC were precisely "on-resonance" and therefore experienced the greatest enhancement factor, small variations in fabrication parameters or surface chemistry density would result in regions of the PC that were not optimally resonant with the excitation source, resulting in lower enhancement factor. Fundamentally, this effect occurs because small changes in optical density on the PC surface result in a shift

Manuscript received May 31, 2011; revised September 12, 2011; accepted September 14, 2011. This work was supported in part by SRU Biosystems, in part by the National Science Foundation (CBET 07-54122), and in part by the National Institutes of Health (PHS 1 R01 GM086382). Any opinions, findings, and conclusions or recommendations expressed in this material are those of the authors and do not necessarily reflect the views of the National Science Foundation. The authors would like to thank colleagues from the Nano Sensors Group for their suggestions and input. The associate editor coordinating the review of this paper and approving it for publication was Prof. Julian Chan.

V. Chaudhery is with the Department of Electrical and Computer Engineering, University of Illinois at Urbana–Champaign, Urbana, IL 61820 USA (e-mail: vchaudh3@illinois.edu).

M. Lu and S.C. Schulz are with SRU Biosystems, Woburn, MA 01801 USA (e-mail: mlu@srubiosystems.com; sschulz@srubiosystems.com).

A. Pokhriyal, is with the Department of Physics, University of Illinois at Urbana–Champaign, Urbana, IL 61820 USA (e-mail: pokhriy1@illinois.edu).

B. T. Cunningham is with the Department of Electrical and Computer Engineering and the Department of Bioengineering, University of Illinois at Urbana–Champaign, Urbana, IL 61820 USA (e-mail: bcunning@illinois.edu).

Color versions of one or more of the figures in this paper are available online at http://ieeexplore.ieee.org.

Digital Object Identifier 10.1109/JSEN.2011.2169401

in reflected wavelength (for a fixed illumination angle) – an effect that has been used effectively for PC-based label free detection [11]–[19]. When considering the use of PCEF surfaces for multiplexed assays using an array of immobilized biomolecule capture spots, this problem is especially critical because the resonant conditions on the PCEF surface are substantially modified by the optical density associated with the capture molecules. This phenomenon results in a situation in which the conditions for optimal enhanced excitation can be substantially different from spot-to-spot within a microarray.

In this paper, we begin by characterizing the field enhancement capability of PCEF surfaces excited by laser beams with different degrees of divergence. A numerical scheme is derived to evaluate the field enhancement factor of PCEF surfaces in Section II. Our results quantify how the fluorescence signal enhancement on the PCEF surface directly benefits from using a collimated excitation beam, and confirms that optimal coupling for enhanced excitation occurs for only a narrow range of incident angles for a fixed excitation wavelength. Focused illumination is shown to also provide effective enhanced excitation with a lower enhancement factor than collimated illumination, while providing greater tolerance to variation of the PC. Our results also show that the Q-factor of the resonance can be effectively controlled through modulation of the PC grating depth. In Section III, these effects are demonstrated experimentally through characterization of a PCEF surface with deposited spots of dye-labeled peptides. Collimated illumination is used to obtain enhancement factors of over 600 × while an enhancement factor of only 30 × is measured on the same device using a commercially available confocal laser scanner. In Section IV, we demonstrate a solution to the fundamental problem of PC surface optical density uniformity by implementing a novel approach that gathers fluorescent images for a range of angles, scanned in small increments. Software is able to select the optimal resonant coupling angle on a pixel-by-pixel basis to construct a fluorescent image in which every region on the PC surface is measured with the highest possible enhancement factor. The method was applied to a 1×3 in^2 PCEF surface.

II. Coupling of PC Sensor and Excitation Light

The PC is a periodic arrangement of dielectric materials with sub-wavelength period, where the device reflects $\sim 100\%$ of the incident light at a specific wavelength and a specific angle [20]–[23]. The theory by which dielectric grating structures with subwavelength period can create resonant reflection spectra was first developed by Hessel and Oliner in 1965 [20] and later attributed to the formation of strong surface standing waves by subsequent analysis by Mashev and Popov [21]–[23]. A subset of these structures later came to be called "Resonant Waveguide Gratings" or "Guided Mode Resonance Filters" but those designed specifically to prevent lateral waveguiding of light at the resonant wavelength and that possess an optical band gap are often referred to as "Photonic Crystals."

The wavelength and angle that match the coupling condition are defined as the resonant wavelength (λ_r) and the resonant angle (θ_r). When the coupling conditions are satisfied, the resonant mode confined near the sensor surface is excited, and exhibits amplified field intensity [21]–[23], which enhances

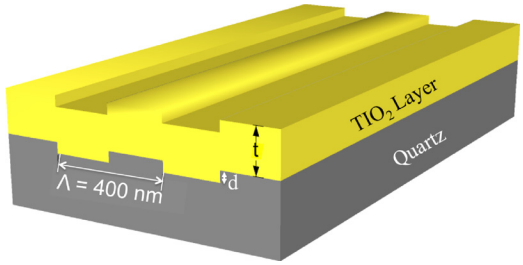

Fig. 1. Schematic diagram of a PC sensor. The grating structure is etched into quartz substrate with period and duty cycle of 400 nm and 50%, respectively.

the fluorescent dye emission immobilized within a 200 nm region above PC surface [24]. Unlike evanescent coupled optical micro- or nano-resonators [25], [26], which require highly precise position control, input light is coupled into PC resonator mode via angle and wavelength control. When most of excitation beam is coupled into resonant mode, the near field strength becomes strong and consequently the PC sensor provides fluorescence enhancement. However, in case of weak coupling, the PC enhancement effect is substantially diminished. A laser (He-Ne, $\lambda = 632.8$ nm) is used to excite a specific fluorophore in our study. Therefore, the resonant wavelength of the PC surface was designed to overlap with the laser emission wavelength by tuning the angle of incidence.

A. Photonic Crystal Sensor Design

Fig. 1 shows a schematic model of the PC structure, which is comprised of a quartz substrate with the top surface etched to provide a periodic refractive index modulation. On top of the grating, a high refractive index thin film of titanium oxide (TiO_2) is deposited as wave guidance layer. The introduced periodic modulation allows for phase-matching of an external incident beam into leaky resonant modes that can be re-radiated into free space [6], [21]–[23], [27]. The λ_r, θ_r, and bandwidth of the resonant mode can be controlled through proper selection of the grating period (Λ), grating depth (d), and thickness of the high index layer (t) depicted in Fig. 1 [28].

The goal of designing the PC surface for fluorescence enhancement is to produce a strongly enhanced near field. A high Q-factor (i.e., narrow bandwidth) PC structure is desirable to improve near field intensity [24]. In a 1D PC structure, the major contributor to energy loss is out-of-plane scattering by the grating structure. To improve cavity Q-factor and to enhance near field intensity, a PC structure with smaller index modulation strength is desirable. Shallower grating depth reduces the out of surface coupling and significantly improves Q-factor. To examine the relationship between Q-factor and grating depth, an RCWA software package (Diffract MOD, RSOFT Design) was used to calculate the transmission efficiency as a function of illumination angle An incident beam of λ_r and θ_r can be coupled into a resonant mode, resulting in a dip in the transmission efficiency, as measured in the far field. PC structures with three different grating depths (15 nm, 30 nm, and 100 nm) were studied. For all three PC structures, the grating period is $\Lambda = 400$ nm while the TiO_2 thickness was selected to maintain a resonant angle of 10° at a resonant wavelength of 633 nm ($t_{TiO_2} = 155$ nm, 158 nm and 185 nm).

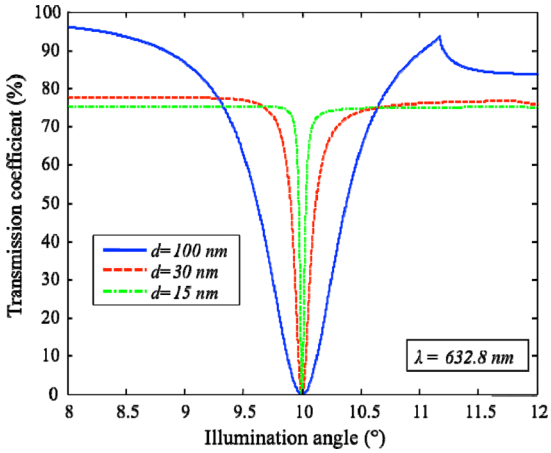

Fig. 2. Simulated transmission spectra of three different PC designs. The PC grating has depth of 15 nm, 30 nm, and 100 nm, respectively. The period of the grating is 400 nm and the TiO_2 thickness is 155 nm, 158 nm, and 185 nm, respectively, to maintain a constant angle of resonant coupling for a wavelength of $\lambda = 632.8$ nm.

The angle transmission spectra are shown in Fig. 2. As expected, using shallower grating depth increases the Q-factor. However, as the Q-factor increases, the coupling condition becomes more stringent. For example, the angle tolerance of a $d = 100$ nm grating is 0.76° but the angle acceptable range of a $d = 15$ nm grating is only 0.06°. In order to fully utilize the field enhancement capability of high Q-factor PC surfaces, the illumination must be well collimated.

B. Resonant Field Distribution in Case of Diverged Beam Excitation

Unfocused laser beams are highly collimated, but exhibit divergence that results in incident angle components with a Gaussian distribution around normal. It is particularly important to note that commercially available fluorescence laser scanners use a focused laser beam [29]–[31]. As we move towards higher Q-factors for PCEF, the angle tolerance for exciting a resonant mode decreases. Therefore, it is important to consider the beam divergence of the excitation light for optimal performance.

To quantify how beam divergence affects the enhancement factor, we developed a calculation scheme. A commercially available Rigorous Coupled Wave Analysis (RCWA) solver (RSoft DiffractMod) can only output the field distribution in a PC that is excited by a plane wave. For simulating real laser excitation conditions, we combined an analytical approach with RCWA to provide a field intensity distribution for a PC surface illuminated by any diverging beam.

We define the z axis as out of the plane of the sensor surface. The total near field amplitude distribution $\mathrm{E(x,z)}$ is averaged for a field distribution at a specific angle θ_j (j is an integer from 0 to n, where n is the total number of incident angles being simulated) weighted by the intensity of the excitation beam $\mathrm{I}(\theta_j)$. The field distribution at an individual angle, $\mathrm{E}_{\theta j}(x,z)$, is calculated using RCWA. The expression of $\mathrm{E(x,z)}$ is given by,

$$\mathrm{E(x,z)} = \sum_{j=0}^{n} \mathrm{I}(\theta_j)\mathrm{E}_{\theta_j}(x,z). \tag{1}$$

The Spatial Intensity distribution of a Gaussian beam propagating along the z-axis is given by,

$$\mathrm{I(x,z)} = \mathrm{I}_0\left[\frac{w_0}{w(z)}\right]^2 e^{-\left(2x^2/w^2(z)\right)}. \tag{2}$$

where w_0 and $w(z)$ represent the minimum spot size and spot size at z, respectively [32].

In order to find the intensity distribution in terms of angle, the spatial distribution function is transformed into k-space governed by $\mathrm{I(x,z)} \langle = \rangle \mathrm{I}(\theta, z)$. The expression of the angle dependent intensity distribution function is

$$\mathrm{I}(\theta) = \mathrm{I}_0\sqrt{\frac{\pi}{2}}\left[\frac{w_0}{w(z)}\right]^2 e^{-(1/2)\left((k_0 \sin\theta)^2 (w^2(z)/8)\right)}. \tag{3}$$

After focusing by a lens with a focal length f, the angle intensity distribution is given by

$$\mathrm{I}(\theta) = \mathrm{I}_0' e^{-(1/2)((k_0 \sin\theta)(\lambda f/\pi L))^2}. \tag{4}$$

where L represents the diameter of the laser beam. In the case of beam illumination at the resonant angle θ_r , (4) can be written as

$$\mathrm{I}(\theta - \theta_r) = \mathrm{I}_0' e^{-(1/2)\left((1/\pi)^2 F^2 k_0^2 \sin^2(\theta-\theta_r)\right)}. \tag{5}$$

where $F = f/L$. Substituting (5) into (1), the averaged field amplitude is given by

$$\mathrm{E(x,z)} = \sum_{j=0}^{n} \mathrm{I}(\theta_j - \theta_r)\mathrm{E}_{\theta_j}(x,z). \tag{6}$$

C. Simulation of Field Enhancement Factor

Using the developed numerical methods, we evaluated the field enhancement factor for the PC structures. Since the resonant angle of the PC surfaces are designed for an incident angle of $\theta = 10°$, the RCWA was used to calculate field distributions in one period of the PC for $0° < \theta < 20°$ with increments of 0.01°. The illumination intensity at a particular angle (θ_j) is calculated using (5) and multiplied with the field amplitude distribution, $\mathrm{E}_{\theta j}(x,z)$ which was simulated using RCWA. The averaged field intensity was found by taking the square of $\mathrm{E(x,z)}$. Since the PC enhancement is a near field effect that is localized to the vicinity of sensor surface, only the field intensity within a 50 nm region above surface is counted. The ratio of the averaged field intensity as compared to the intensity on a reference glass slide is defined as the enhancement factor. Assuming a laser spot with 1 mm diameter, the divergence of the beam after focusing can be altered using a lens with different focal lengths. In our simulation, we consider the laser beam with divergence between 3.3° to 0.00033°. As shown in Fig. 3, when the excitation beam is highly diverging, the enhancement factor of a low Q-factor PC is higher than that of the high Q-factor PC. However, the high Q-factor PC exhibits an enhancement factor of 263 × if the excitation beam becomes more collimated. An excitation beam with angle of divergence beyond 0.005° can be fully coupled into the resonance. An excessively collimated beam will not result in a better enhancement factor once the coupling condition is met.

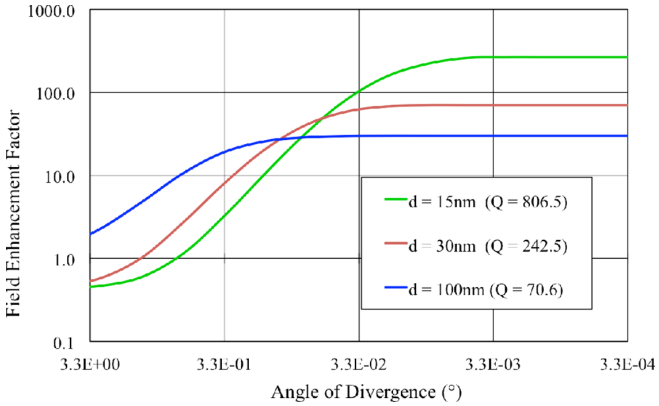

Fig. 3. Simulated local field enhancement factor in terms of angle divergence of the excitation laser beam for PC substrates with different Q-factors.

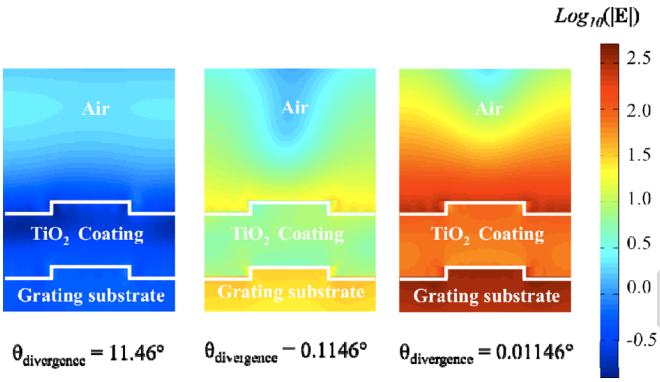

Fig. 4. Simulated local field enhancement factor in terms of angle divergence of the excitation laser beam for PC surfaces with different angle of divergence for a 15 nm depth grating.

To further illustrate the field enhancement effect, the averaged near field intensities of gratings with depth $d = 15$ nm were calculated and compared in Fig. 4 for three exemplary excitation beams with divergence of 11.46°, 0.1146°, and 0.01146°. We investigate the effect of variations in excitation beam divergence to near field strength. In Fig. 4, the field distribution in a single period of the PC structure is plotted at the resonant wavelength. The white contour highlights the surface of the grating substrate and the top of the PC surface. Fig. 4(a) demonstrates the field intensity distribution at laser beam divergence of 11.46°. Compared to the mode profile given in Fig. 4(a), the near field shown in Fig. 4(b) is ~ 60 times stronger when the excitation beam is less divergent (0.1146°). For the case of least divergence shown in Fig. 4(c), the field intensity is highest (~ 507 times higher than the most divergent case). This example illustrates that using a highly collimated excitation source is critical to achieving the greatest enhanced near field.

III. PC Enhanced Fluorescence Instrumentation

Two different types of fluorescence detection systems were studied for PCEF: a commercially available microarray laser scanner and a modified fluorescence microscope that is specifically designed for PCEF. The apparatus of the microarray laser scanner (LS Reloaded, Tecan Inc.) is shown in Fig. 5(a). This system uses a focused laser beam (beam divergence $\sim 2.5°$) as the excitation source and a photomultiplier tube (PMT) as

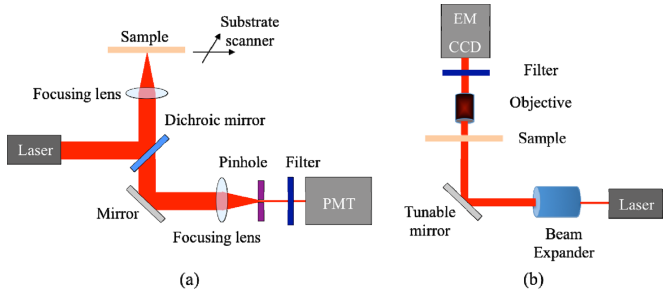

Fig. 5. (a) Schematic diagram of optical setup of the confocal laser scanner and (b) schematic drawing of PC enhanced fluorescence microscope. (a) Microarray laser scanner. (b) PC enhanced fluorescence microscope.

the fluorescence signal detector. In order to form an image, the substrate is scanned and the fluorescence signal intensity for each pixel is acquired. The apparatus of the custom-built fluorescent detection system, which is referred as the PC Enhanced Fluorescence Microscope (PCEFM), is shown in Fig. 5(b). In the PCEFM system, the fluorescent sample is imaged by an electron multiplying charge coupled device (EMCCD; Hammamatsu Inc.) via a 4 × microscope objective (numerical aperture N.A. = 0.1). Unlike the confocal laser scanner, the PCEFM works in the imaging mode, which significantly improves the measurement throughput. For both systems, a HeNe laser ($\lambda = 632.8$ nm) is used as an excitation light source, and a bandpass filter is placed in front of the detectors to reject excitation laser light.

The microarray laser scanner uses a lens with a high numerical aperture (N.A.) to focus the laser beam on to the sample and collects the fluorescence signal resulting from this excitation. Due to the focusing effect, the illumination laser beam angle spans from 0° to 30°. As a result, only a small portion of the excitation energy can be coupled into the resonant mode of the PC surface, thus compromising the enhancement performance of the PC. For the PC surface with $Q \sim 300$, the coupling efficiency is less than 20%. As discussed above, in order to take full advantage of a PC and accomplish high enhancement of the fluorescence signal, it is critical to achieve a good coupling efficiency between the excitation laser beam and the PC surface. The PCEFM setup is designed specifically to achieve this and utilizes collimated illumination for this purpose. As shown in Fig. 5(b), the output of the HeNe laser is expanded to produce a beam with diameter of 20 mm and divergence of 0.037° using a beam expander. In order to accurately control the angle of incidence, the PCEFM system utilizes a high precision angle tuning gimbal-mounted mirror which is itself is mounted on a motorized linear stage that moves as the mirror rotates. The movement of this linear stage compensates the beam shift due to incident angle variation and thereby ensures a fixed illumination area. The angle tuning resolution of this configuration is 0.005°, resulting in the capability for testing PC devices with angle bandwidth as narrow as 0.01°. A coupling efficiency of 98% has been achieved using this system with a PC surface with angle bandwidth of 0.3°.

IV. Coupling of PC Sensor and Excitation Light

The PC sensor used in this paper was fabricated using nanoimprint lithography (NIL) [33], [34]. The detailed fabrication

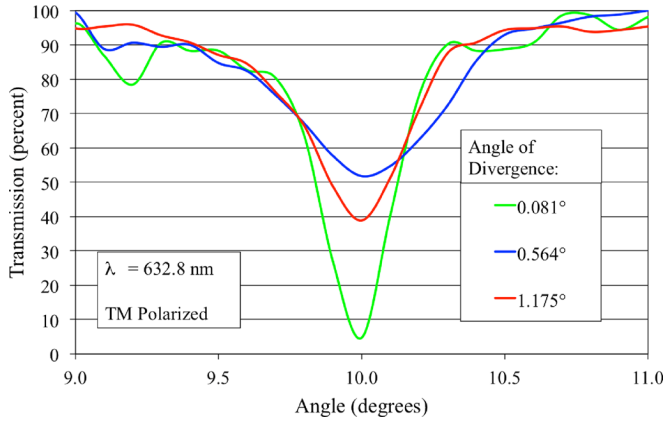

Fig. 6. Transmission spectrum of a PC enhancement substrate where the resonant angle is around 10°. The illumination spot is has divergence of 1.175°, 0.564°, and 0.081°.

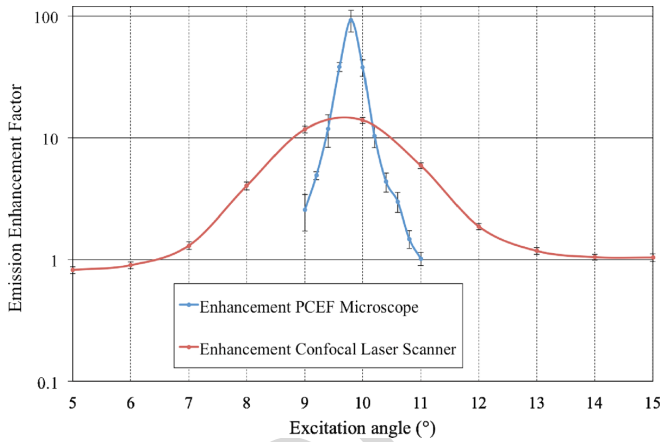

Fig. 7. Comparison of the fluorescence intensity as a function of excitation angle measured using the PCEF microscope and the Confocal Laser Scanner.

procedure has been fully described in a previous publication [35]. The fabricated PC structure has a period of $\Lambda = 400$ nm, duty cycle of 50%, and grating depth of $\mathrm{d} = 40$ nm. As a high index layer, 130 nm of TiO_2 was coated by RF-sputtering. Illuminated by a HeNe laser at $\lambda = 632.8$ nm, this PC exhibits resonance at an angle of $\theta = 10°$. The coupling between the PC resonant mode and laser beam with different degrees of divergence was investigated. The enhancement capability of the PC was compared between the confocal laser scanner and the PCEFM.

A. *Transmission Spectrum*

In order to show the effect of laser beam divergence on the coupling between the PC and excitation light, we measured the transmission spectrum using focused and non-focused beams as illumination sources. To measure the transmission spectrum in terms of angle, the sample was illuminated by a HeNe laser and the transmitted light power was monitored by a silicon photodetector while the angle of incidence was scanned around the resonant angle (9° to 11.5°). Low transmission (high reflection) efficiency indicates good coupling of incident light into the resonant mode of the PC. By using lenses of different focal lengths, we varied the divergence of the incident laser beam. Without a focusing lens, the divergence angle is 0.081°, using lenses with focal lengths of 125 mm and 60 mm, the beam divergences are 0.564° and 1.175°, respectively. As shown in Fig. 6, the measured transmission spectra were compared for the collimated and non-collimated illumination. Using a collimated laser beam, the transmission efficiency was 5% at resonant angle with angle full-width half maximum of 0.37°. The transmission efficiency increases to 39% and 51% when the laser beam was focused by lenses with 125 mm and 60 mm focal lengths, respectively. Due to the broadening of incidence angle, a lower percentage of excitation energy is coupled into resonance, and transmission efficiency becomes higher. With regard to PC enhanced fluorescence, the diverged beam results in only a portion of the excitation energy being amplified by the PC resonance, which diminishes the fluorescence enhancement capability of the PC sensor.

B. *Enhanced Fluorescence Intensity*

Having established a clear relationship between degree of collimation of incident light and coupling efficiency with a PC, we performed fluorescence measurements to experimentally correlate the influence of degree of collimation of incident light with the extent of fluorescence enhancement. We used the microarray laser scanner and the PCEFM discussed in Section III, to represent cases for focused and collimated light. The signal enhancement factor for the on-resonance case with respect to the off-resonance case was measured over a range of angles around the resonance angle. This is shown in Fig. 7.

The collimated light gave a signal enhancement factor almost $7\times$ higher than the case for the focused light. This can be easily explained as a direct consequence of the higher magnitude of surface localized electric field intensity that interacts with fluorophores immobilized on the surface of the PC.

Another interesting observation was that the signal enhancement is much more sensitive to the proximity to the resonance angle for collimated excitation ($\mathrm{FWHM}_\theta < 0.4°$) when judged against focused excitation (peak $\mathrm{FWHM}_\theta > 1.5°$). This can be explained as a consequence of the sensitivity of the coupling efficiency of the PC to change in excitation angle for collimated light. Thus, for the PCEFM a small deviation from the resonance condition will result in a large drop in the surface localized electric field intensity, ultimately leading to lower enhancement in fluorescence intensity. For the case of focused light, since the incident beam consists of a spread of angles, over a fairly large range there will be some amount of light that will always be present in the resonant angle range. Thus, even though the coupling will never be as efficient and the electric field intensities will never reach high values, the fluorescence enhancement will have a much greater angle tolerance. Thus the degree of collimation of the excitation light (which influences the coupling efficiency of the PC as described in the previous section) is the ultimate determining factor for the degree of enhancement. The sensitivity of the degree of enhancement to the proximity to the resonance angle has far-reaching implications for performing multiplexed assays on a PC surface.

For relating our enhancement factors on the PC to a glass slide we performed a study to analyze the total enhancement of the PC on-resonance when compared to unpatterned glass. Fig. 8 shows a bar graph plot for the signal enhancement as measured on the PCEFM and the confocal laser scanner. The plot shows a very high signal enhancement for the on-resonance case compared to the off-resonance case ($169\times$ for PCEFM, and $15\times$

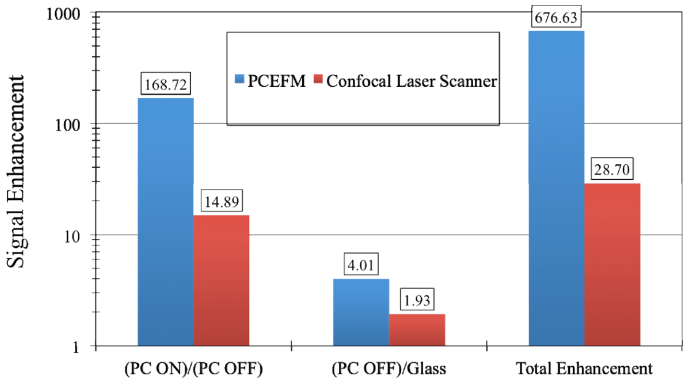

Fig. 8. Comparison of the fluorescence enhancement using the PCEF microscope and the Confocal Laser Scanner. The fluorescence signal enhancement for the PC on resonance compared to the off resonance case is attributed to the "enhanced excitation" property of the PC. The fluorescence signal enhancement for the PC off resonance compared to unpatterned glass is attributed to the "enhanced extraction" property of the PC. The total enhancement is the ratio of the fluorescence signal for the PC on resonance to the unpatterned glass.

for the laser scanner) which is due to the enhanced excitation effect. The off-resonance case for the PC also has a higher signal as compared to a glass slide ($\sim 4\times$ for the PCEFM and $\sim 2\times$ for the laser scanner). This is a result of the PC enhanced extraction effect [14]. In this case, emitted photons, which would ordinarily exit the surface distributed uniformly in all directions, are spatially biased away from the PC surface at an (approximately) normal angle, so they may be gathered more efficiently by the detection optics.

The combination of the two enhancement effects provides a net signal enhancement (compared to unpatterned glass) of $\sim 677\times$ using the PCEFM and $\sim 29\times$ using the laser scanner.

C. Angle-Scanned Image Optimization

Having established the superior performance of a PC under collimated conditions and the promise of high enhancement offered by the PCEFM, it is necessary to provide a uniform enhancement effect over substantial surface areas, such as those used for protein microarrays or DNA microarrays that are comprised of hundreds or thousands of capture spots. Because the enhancement factor is highly sensitive to the angle of incidence for a collimated beam (Fig. 7), small variations in the PC surface resonant coupling angle caused by nonuniformities in the PC structure (for example, the TiO_2 layer thickness) and the density of surface functionalization layers will result in substantial variations in fluorescent intensity if a fixed incident angle is used to scan the entire device. This problem is further complicated by the variable density of immobilized capture molecules, such as DNA or antibodies that are deposited as arrays of spots on the PC surface. Capture molecules are typically deposited with high density, and therefore result in a substantially lower PC coupling angle compared to the regions of the surface between capture spots. There is thus no single incident angle that can be used to optimally couple a laser to every region of a PC surface.

In order retain the benefits of signal enhancement while still performing fast high throughput measurements; we developed a methodology to account for the variation in the resonant coupling angle across the device. Rather than gathering fluorescent

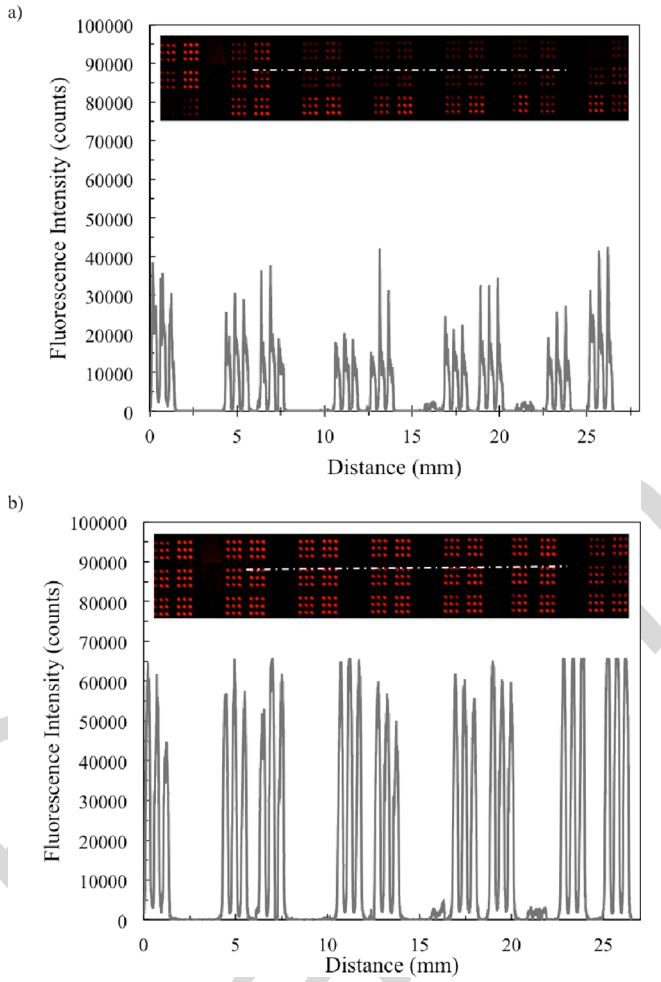

Fig. 9. Intensity profile as a function of distance for a line of fluorescent image pixels profiling spots of Alexa-647 conjugated PPL for the PC: (a) using a fixed excitation angle at 10° and (b) the fluorescence intensity is scanned at 11 angles near the resonance angle. The scanned images are shown in insets.

output images with the PCEFM using a single incident angle, we capture a sequence of fluorescence images over a range of angles that always includes the resonance angle. Software is used to compare the images taken at each angle, and to select the maximum intensity of every pixel over the scanning range. Because the maximum intensity for any pixel will always be generated when the incident angle matches the optimal resonant condition, a new image can constructed using the maximum intensity angle for each pixel.

To demonstrate the angle-scanning method, a 3×3 array of Poly(Lys, Phe) conjugated with Alexa-647 (Invitrogen) was spotted at a concentration of 9.9 $\mu g/ml$ onto the 1×3 in^2 PC surface by a piezoelectric dispenser (Piezorray, Perkin Elmer) with a center-to-center separation of 500 μm and a spot radius of ~ 200 μm. Prior to spotting, the PC surface was pre-cleaned with O_2 plasma for 3 min. and then cleaned by sonication in acetone, isopropanol and deionized (DI) water and followed by drying under a nitrogen stream. After spotting, the PC was incubated for 24 hours in a sealed container. The spot densities were selected so as to give an approximate shift of $-0.2°$ in the PC coupling condition.

Selecting a single incident angle of $\theta = 10°$, the PCEFM gathered the image shown in Fig. 9(a). Using a $4\times$ microscope

objective, a single fluorescent image has a field of view of $\sim 2 \times 2\ \mathrm{mm}^2$. An automated motion stage enables capture of fluorescent images from adjacent regions, and concatenation of images results in a fluorescent image of the entire slide, using a total scanning time of 24 seconds. Nominally, each spot in the array is identical, but the fluorescent intensity shows the effects of nonoptimal laser coupling to the PC resonance in several regions of the chip, resulting in a coefficient of variability of $\mathrm{CV} = 51\%$ for the on-spot intensity.

Fig. 9(b) is a fluorescence image of the same slide as Fig. 9(a) with the image constructed by the new methodology. For each imaged region, a sequence of fluorescence intensity images is gathered from $9.5^\circ < \theta < 10.5^\circ$ in 0.1° increments, for a total of 11 images per frame. By gathering the additional images, the scanning time for the entire $1 \times 3\ \mathrm{in}^2$ area increased to 48 sec. The maximum-pixel selection and composite image-processing algorithm runs in 60 sec. As a result of the new method, the spot CV is reduced to 17.9%. This level of spot-to-spot variability is consistent with what is typically obtained for fluorescent images of spot intensities on glass surfaces (data not shown), and therefore represents variability due to the spots themselves, rather than variability in the detection method. Using the angle scanning approach, we observe a consistently high enhancement factor across the entire PC area.

V. Conclusion

We have reported on the study of PC enhanced fluorescence illuminated with laser beams with different degrees of divergence. By use of an imaging system that enables angle-tunable collimated illumination of the PC surface, we have established improved performance for PC when subjected to collimated excitation as compared to focused excitation in a confocal laser scanner, demonstrating raw signal enhancement of 677 $\times$. The signal enhancement is accompanied by an extreme sensitivity to the angle of excitation. This results in a problem of variability when attempting to utilize the PCEFM for high throughput measurements, such as those used in DNA microarrays or protein microarrays. In order to address this issue, an angle-scanning method was developed that allows optimal coupling to every pixel in a PC-based fluorescent image, and thus achieves a uniformly high enhancement factor over large surface areas.

References

[1] J. W. Lichtman and J.-A. Conchello, "Fluorescence microscopy," *Nature Methods*, vol. 2, no. 12, p. 910(10), 2005.

[2] J. Stenken, "Introduction to fluorescence sensing," *J. Amer. Chem. Soc.*, vol. 131, no. 30, p. 10791, 2009.

[3] W. Budach *et al.*, "Generation of transducers for fluorescence-based microarrays with enhanced sensitivity and their application for gene expression profiling," *Anal. Chem.*, vol. 75, pp. 2571–2577, 2003.

[4] H. Jin and R. C. Zangar, "Protein modifications as potential biomarkers in breast cancer," *Biomarker Insights*, vol. 2009, no. 1761, p. 191, 2009.

[5] P. C. Mathias, H.-Y. Wu, and B. T. Cunningham, "Employing two distinct photonic crystal resonances to improve fluorescence enhancement," *Appl. Phys. Lett.*, vol. 95, no. 2, p. 021111, 2009.

[6] N. Ganesh *et al.*, "Leaky-mode assisted fluorescence extraction: Application to fluorescence enhancement biosensors," *Opts. Exp.*, vol. 16, no. 26, pp. 21626–21640, 2008.

[7] I. D. Block *et al.*, "A detection instrument for enhanced-fluorescence and label-free imaging on photonic crystal surfaces," *Opt. Exp.*, vol. 17, no. 15, pp. 13222–13235, 2009.

[8] H. Y. Wu *et al.*, "Magnification of photonic crystal fluorescence enhancement via TM resonance excitation and TE resonance extraction on a dielectric nanorod surface," *Nanotechnology*, vol. 21, no. 12, pp. 125–203, Mar. 2010.

[9] P. C. Mathias, H.-Y. Wu, and B. T. Cunningham, "Employing two distinct photonic crystal resonances for improved fluorescence enhancement," *Appl. Phys. Lett.*, vol. 95, no. 2, p. 021111, 2009.

[10] P. C. Mathias, N. Ganesh, and B. T. Cunningham, "Application of photonic crystal enhanced fluorescence to a cytokine immunoassay," *Anal. Chem.*, vol. 80, no. 23, pp. 9013–9020, 2008.

[11] B. T. Cunningham *et al.*, "A plastic colorimetric resonant optical biosensor for multiparallel detection of label-free biochemical interactions," *Sens. Actuators B*, vol. 85, no. 3, pp. 219–226, 2002.

[12] I. D. Block, L. L. Chan, and B. T. Cunningham, "Photonic crystal optical biosensor incorporating structured low-index porous dielectric," *Sens. Actuators B*, vol. 120, no. 1, pp. 187–193, Dec. 2006.

[13] B. T. Cunningham *et al.*, "Label-free assays on the BIND system," *J. Biomolecular Screening*, vol. 9, pp. 481–490, 2004.

[14] B. T. Cunningham and L. L. Laing, "Label-free detection of biomolecular interactions: Applications in proteomics and drug discovery," *Expert Reviews in Proteomics*, vol. 3, no. 3, pp. 271–281, 2006.

[15] L. Chan *et al.*, "A label-free photonic crystal biosensor imaging method for detection of cancer cell cytotoxicity and proliferation," *Apoptosis*, vol. 12, no. 6, pp. 1061–1068, 2007.

[16] L. L. Chan *et al.*, "Label-free imaging of cancer cells using photonic crystal biosensors and application to cytotoxicity screening of a natural compound library," *Sens. Actuators B*, vol. 132, pp. 418–425, 2008.

[17] L. L. Chan *et al.*, "A self-referencing method for microplate label-free photonic crystal biosensors," *IEEE Sensors J.*, vol. 6, no. 6, pp. 1551–1556, Dec. 2006.

[18] L. L. Chan *et al.*, "General method for discovering inhibitors of protein-DNA interactions using photonic crystal biosensors," *ACS Chem. Biol.*, vol. 3, no. 7, pp. 437–448, 2008.

[19] P. Li *et al.*, "A new method for label-free imaging of biomolecular interactions," *Sens. Actuators B, Chem.*, vol. 99, pp. 6–13, 2004.

[20] A. Hessel and A. A. Oliner, "A new theory of Wood's anomalies on optical gratings," *Appl. Opt.*, vol. 4, no. 10, pp. 1275–1297, 1965.

[21] E. Popov, L. Mashev, and D. Maystre, "Theoretical-study of the anomalies of coated dielectric gratings," *Optica Acta*, vol. 33, no. 5, pp. 607–619, May 1986.

[22] L. Mashev and E. Popov, "Diffraction efficiency anomalies of multicoated dielectric gratings," *Opt. Commun.*, vol. 51, no. 3, pp. 131–136, 1984.

[23] L. Mashev and E. Popov, "Zero order anomaly of dielectric coated gratings," *Opt. Commun.*, vol. 55, no. 6, pp. 377–380, 1985.

[24] N. Ganesh *et al.*, "Distance dependence of fluorescence enhancement from photonic crystal surfaces," *J. Appl. Phys.*, vol. 103, p. 083104, 2008.

[25] P. Kramper *et al.*, "Direct spectroscopy of a deep two-dimensional photonic crystal microresonator," *Phys. Rev. B*, vol. 64, no. 23, p. 233102, 2001.

[26] C. J. Barrelet *et al.*, "Hybrid single-nanowire photonic crystal and microresonator structures," *Nano Lett.*, vol. 6, no. 1, pp. 11–15, Jan. 2006.

[27] P. C. Mathias *et al.*, "Graded wavelength one-dimensional photonic crystal reveals spectral characteristics of enhanced fluorescence," *J. Appl. Phys.*, vol. 103, p. 094320, 2008.

[28] I. D. Block *et al.*, "A sensitivity model for predicting photonic cyrstal biosensor performance," *IEEE Sensors J.*, vol. 8, no. 3, pp. 274–280, Mar. 2008.

[29] K. J. Halbhuber and K. Konig, "Modern laser scanning microscopy in biology, biotechnology and medicine," *Ann. Anatomy-Anatomischer Anzeiger*, vol. 185, no. 1, pp. 1–20, Jan. 2003.

[30] W. B. Amos and J. G. White, "How the confocal laser scanning microscope entered biological research," *Biol. Cell*, vol. 95, no. 6, pp. 335–342, 2003.

[31] S. Paddock, "Over the rainbow: 25 Years of confocal imaging," *BioTechniques*, vol. 44, no. 5, pp. 643–648, 2008.

[32] B. E. A. Saleh and M. C. Teich, *Fundamentals of Photonics*, 1st ed. New York: Wiley, 1991, pp. 80–107.

[33] S. Y. Chou, P. R. Krauss, and P. J. Renstrom, "Imprint of sub-25 nm vias and trenches in polymers," *Appl. Phys. Lett.*, vol. 67, no. 21, pp. 3114–3116, 1995.

[34] S. Y. Chou, P. R. Krauss, and P. J. Renstrom, "Imprint lithography with 25-nanometer resolution," *Science*, vol. 272, no. 5258, pp. 85–87, Apr. 1996.

[35] A. Pokhriyal *et al.*, "Photonic crystal enhanced fluorescence using a quartz substrate to reduce limits of detection," *Opt. Exp.*, vol. 18, no. 24, pp. 24793–24808, 2010.

Vikram Chaudhery received the B.S. and M.S. degrees in electrical and computer engineering from the University of Illinois at Urbana–Champaign, Urbana, in 2009 and 2011, respectively. Currently, he is working towards the Ph.D. degree as a Graduate Research Assistant under the direction of Prof. Brian T. Cunningham at the University of Illinois at Urbana–Champaign.

His research focuses on the design, characterization and optimization of novel detection and imaging instrumentation for photonic crystal biosensors and its application in life sciences.

Meng Lu received the B.S. degree in electrical and computer engineering from University of Science and Technology of China, Beijing, in 2002, and the M.S. and Ph.D. degrees in electrical and computer engineering from the University of Illinois at Urbana–Champaign, Urbana, in 2004 and 2008, respectively.

His research at the University of Illinois at Urbana–Champaign under the direction of Prof. Brian T. Cunningham focused on the development of optical sensor systems. He is currently with SRU Biosystems, Woburn, MA, working on optical biosensors.

Anusha Pokhriyal received the M.S. degree in physics from Worcester Polytechnic Institute, Worcester, MA, in 2008. She is currently working towards the Ph.D. degree as a Graduate Research Assistant under the direction of Prof. Brian T. Cunningham at the University of Illinois at Urbana–Champaign, Urbana.

Her research focuses on the design and characterization of optical biosensors and device fabrication processes.

Stephen C. Schulz, photograph and biography not available at the time of publication.

Brian Cunningham received the B.S., M.S., and Ph.D. degrees in electrical and computer engineering from the University of Illinois at Urbana–Champaign, Urbana. His thesis research was in the field of optoelectronics and compound semiconductor material science, where he contributed to the development of crystal growth techniques that are now widely used for manufacturing solid state lasers, and high-frequency amplifiers for wireless communication.

He is a Professor in the Department of Electrical and Computer Engineering and the Department of Bioengineering at the University of Illinois at Urbana–Champaign, where he has been a faculty member since 2004. His group focuses on the development of nanophotonic surfaces, plastic-based nanofabrication methods, and novel instrumentation approaches for biodetection with applications in pharmaceutical screening, life science research, environmental monitoring, disease diagnostics, and point-of-care patient testing. At the University of Illinois at Urbana–Champaign, he serves as the Director of the Bioengineering Graduate Program and Director of the NSF Center for Agricultural, Biomedical, and Pharmaceutical Nanotechnology (CABPN). He is a founder and the Chief Technical Officer of SRU Biosystems, Woburn, MA, a life science tools company that provides high sensitivity plastic-based optical biosensors, instrumentation, and software to the pharmaceutical, academic research, genomics, and proteomics communities. Prior to founding SRU Biosystems in June 2000, he was the Manager of Biomedical Technology at Draper Laboratory, Cambridge, MA, where he directed R&D projects aimed at utilizing defense-related technical capabilities for medical applications. In addition, he served as Group Leader for MEMS Sensors at Draper Laboratory, where he directed a group performing applied research on microfabricated inertial sensors, acoustic sensors, optical switches, microfluidics, tissue engineering, and biosensors. Concurrently, he was an Associate Director of the Center for Innovative Minimally Invasive Therapy (CIMIT), a Boston-area medical technology consortium, where he led the Advanced Technology Team on Microsensors. Before working at Draper Laboratory, he spent five years at the Raytheon Electronic Systems Division developing advanced infrared imaging array technology for defense and commercial applications.

Prof. Cunningham was recognized with the IEEE Sensors Council 2010 Technical Achievement Award for the invention, development, and commercialization of biosensors utilizing photonic crystals.

Angle-Scanning Photonic Crystal Enhanced Fluorescence Microscopy

Vikram Chaudhery, Meng Lu, Anusha Pokhriyal, Stephen C. Schulz, and Brian T. Cunningham, *Senior Member, IEEE*

***Abstract*—Photonic crystal enhanced fluorescence (PCEF) has been demonstrated as an effective means for amplifying the excitation provided to surface-bound fluorescent molecules while simultaneously enhancing fluorescence emission collection efficiency. Optimal coupling of a fluorophore-exciting light source to the PC occurs with the use of collimated plane waves, as utilized in a special-purpose fluorescence microscope specifically designed for coupling with PCEF surfaces. However, PCEF surfaces are also capable of coupling light from focused sources, such as those used in commercially available confocal laser scanners, but with a reduction in the obtainable enhancement factor. Using computer simulations and experimental measurements, we describe the interaction between the resonant bandwidth of a PCEF device surface and the optical design of the detection instrumentation that is used to provide fluorescence excitation. We show that highly collimated illumination is required for achieving the greatest PCEF enhancement factors, but at the expense of poor tolerance to nonuniformities in resonant wavelength across the PCEF surface. To overcome this limitation, we demonstrate a fixed wavelength/multiple incident angle scanning detection system that is capable of measuring every pixel in a PCEF fluorescence image under conditions that optimize resonant excitation efficiency.**

***Index Terms*—Fluorescence, microscopy, photonic crystals.**

I. Introduction

FLOURESCENCE has emerged as a useful tool for imaging and detection in medical and biological sciences due to its excellent sensitivity, wide availability of dye molecules, ease of application to broad classes of biomolecules, and robust detection instrumentation. The major limitation of fluorescence is the strength of signals that can often limit visualization and quantification of low concentration analytes in numerous fluorescence based assays [1], [2]. To address the need for higher sensitivity and improved signal-to-noise ratios (SNR) in surface-based fluorescence assays, dielectric-based photonic crystal (PC) surfaces have been utilized in the context of gene expression analysis [3], protein biomarker detection [4].

PC surfaces provide a consistent and highly efficient platform for enhancement of fluorescence by exploiting their optical resonance characteristics to provide a heightened excitation field (resulting in a phenomenon called "enhanced excitation") along with the ability to control the photonic dispersion which provides a powerful mechanism to redirect the emitted light into certain preferred directions, where it can be detected with greater efficiency ("enhanced extraction"). The simultaneous implementation of these two techniques has been shown to boost the radiation detected from quantum dots and fluorescent dye molecules by two orders of magnitude [5]–[8].

While the effects of PC enhanced excitation and enhanced extraction can be combined with multiplicative effects [7]–[9] this work is primarily concerned with optimization of enhanced excitation through the interaction of the PC resonant mode characteristics and the degree of collimation of the illumination that is provided to the PC. The enhanced excitation and extraction mechanisms have been shown not to alter the fluorophore lifetime by the Purcell effect [6] when a PC with moderate Q-factor (Q is mathematically defined as $\lambda/\Delta\lambda$, where λ is the resonant wavelength, and $\Delta\lambda$ is the full-width at half maximum of the resonant peak spectrum) is used.

In our previous work, a confocal laser scanner, incorporating a focused laser beam, was used to good effect for PCEF [9], [10]. However, due to the angle selectivity of the PCEF surface, only a portion of the excitation energy can be coupled into the resonance mode and contribute to enhanced fluorescence emission. To improve PCEF performance, we demonstrated the use of a collimated excitation scheme [7], in which the excitation beam matches the resonance angle of the target resonance mode. In the detection instrument described in our previous work, a single excitation angle (at a fixed illumination wavelength) was selected for imaging an entire PC surface. Using this fixed angle/fixed wavelength excitation approach, only limited regions of a high-Q PCEF surface could be optimally excited. While some parts of the PC were precisely "on-resonance" and therefore experienced the greatest enhancement factor, small variations in fabrication parameters or surface chemistry density would result in regions of the PC that were not optimally resonant with the excitation source, resulting in lower enhancement factor. Fundamentally, this effect occurs because small changes in optical density on the PC surface result in a shift

Manuscript received May 31, 2011; revised September 12, 2011; accepted September 14, 2011. This work was supported in part by SRU Biosystems, in part by the National Science Foundation (CBET 07-54122), and in part by the National Institutes of Health (PHS 1 R01 GM086382). Any opinions, findings, and conclusions or recommendations expressed in this material are those of the authors and do not necessarily reflect the views of the National Science Foundation. The authors would like to thank colleagues from the Nano Sensors Group for their suggestions and input. The associate editor coordinating the review of this paper and approving it for publication was Prof. Julian Chan.

V. Chaudhery is with the Department of Electrical and Computer Engineering, University of Illinois at Urbana–Champaign, Urbana, IL 61820 USA (e-mail: vchaudh3@illinois.edu).

M. Lu and S.C. Schulz are with SRU Biosystems, Woburn, MA 01801 USA (e-mail: mlu@srubiosystems.com; sschulz@srubiosystems.com).

A. Pokhriyal, is with the Department of Physics, University of Illinois at Urbana–Champaign, Urbana, IL 61820 USA (e-mail: pokhriy1@illinois.edu).

B. T. Cunningham is with the Department of Electrical and Computer Engineering and the Department of Bioengineering, University of Illinois at Urbana–Champaign, Urbana, IL 61820 USA (e-mail: bcunning@illinois.edu).

Color versions of one or more of the figures in this paper are available online at http://ieeexplore.ieee.org.

Digital Object Identifier 10.1109/JSEN.2011.2169401

in reflected wavelength (for a fixed illumination angle) – an effect that has been used effectively for PC-based label free detection [11]–[19]. When considering the use of PCEF surfaces for multiplexed assays using an array of immobilized biomolecule capture spots, this problem is especially critical because the resonant conditions on the PCEF surface are substantially modified by the optical density associated with the capture molecules. This phenomenon results in a situation in which the conditions for optimal enhanced excitation can be substantially different from spot-to-spot within a microarray.

In this paper, we begin by characterizing the field enhancement capability of PCEF surfaces excited by laser beams with different degrees of divergence. A numerical scheme is derived to evaluate the field enhancement factor of PCEF surfaces in Section II. Our results quantify how the fluorescence signal enhancement on the PCEF surface directly benefits from using a collimated excitation beam, and confirms that optimal coupling for enhanced excitation occurs for only a narrow range of incident angles for a fixed excitation wavelength. Focused illumination is shown to also provide effective enhanced excitation with a lower enhancement factor than collimated illumination, while providing greater tolerance to variation of the PC. Our results also show that the Q-factor of the resonance can be effectively controlled through modulation of the PC grating depth. In Section III, these effects are demonstrated experimentally through characterization of a PCEF surface with deposited spots of dye-labeled peptides. Collimated illumination is used to obtain enhancement factors of over 600 $\times$ while an enhancement factor of only 30 $\times$ is measured on the same device using a commercially available confocal laser scanner. In Section IV, we demonstrate a solution to the fundamental problem of PC surface optical density uniformity by implementing a novel approach that gathers fluorescent images for a range of angles, scanned in small increments. Software is able to select the optimal resonant coupling angle on a pixel-by-pixel basis to construct a fluorescent image in which every region on the PC surface is measured with the highest possible enhancement factor. The method was applied to a 1×3 in^2 PCEF surface.

II. Coupling of PC Sensor and Excitation Light

The PC is a periodic arrangement of dielectric materials with sub-wavelength period, where the device reflects $\sim 100\%$ of the incident light at a specific wavelength and a specific angle [20]–[23]. The theory by which dielectric grating structures with subwavelength period can create resonant reflection spectra was first developed by Hessel and Oliner in 1965 [20] and later attributed to the formation of strong surface standing waves by subsequent analysis by Mashev and Popov [21]–[23]. A subset of these structures later came to be called "Resonant Waveguide Gratings" or "Guided Mode Resonance Filters" but those designed specifically to prevent lateral waveguiding of light at the resonant wavelength and that possess an optical band gap are often referred to as "Photonic Crystals."

The wavelength and angle that match the coupling condition are defined as the resonant wavelength (λ_{r}) and the resonant angle (θ_{r}). When the coupling conditions are satisfied, the resonant mode confined near the sensor surface is excited, and exhibits amplified field intensity [21]–[23], which enhances the fluorescent dye emission immobilized within a 200 nm region above PC surface [24]. Unlike evanescent coupled optical micro- or nano-resonators [25], [26], which require highly precise position control, input light is coupled into PC resonator mode via angle and wavelength control. When most of excitation beam is coupled into resonant mode, the near field strength becomes strong and consequently the PC sensor provides fluorescence enhancement. However, in case of weak coupling, the PC enhancement effect is substantially diminished. A laser (He-Ne, $\lambda = 632.8$ nm) is used to excite a specific fluorophore in our study. Therefore, the resonant wavelength of the PC surface was designed to overlap with the laser emission wavelength by tuning the angle of incidence.

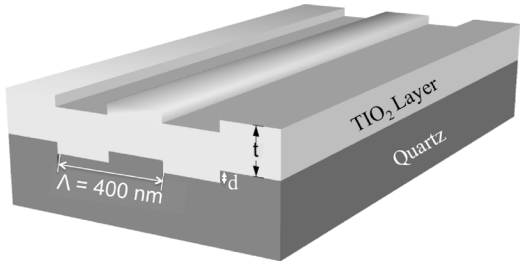

Fig. 1. Schematic diagram of a PC sensor. The grating structure is etched into quartz substrate with period and duty cycle of 400 nm and 50%, respectively.

A. Photonic Crystal Sensor Design

Fig. 1 shows a schematic model of the PC structure, which is comprised of a quartz substrate with the top surface etched to provide a periodic refractive index modulation. On top of the grating, a high refractive index thin film of titanium oxide ($\mathrm{TiO_2}$) is deposited as wave guidance layer. The introduced periodic modulation allows for phase-matching of an external incident beam into leaky resonant modes that can be re-radiated into free space [6], [21]–[23], [27]. The λ_{r}, θ_{r}, and bandwidth of the resonant mode can be controlled through proper selection of the grating period (Λ), grating depth (d), and thickness of the high index layer (t) depicted in Fig. 1 [28].

The goal of designing the PC surface for fluorescence enhancement is to produce a strongly enhanced near field. A high Q-factor (i.e., narrow bandwidth) PC structure is desirable to improve near field intensity [24]. In a 1D PC structure, the major contributor to energy loss is out-of-plane scattering by the grating structure. To improve cavity Q-factor and to enhance near field intensity, a PC structure with smaller index modulation strength is desirable. Shallower grating depth reduces the out of surface coupling and significantly improves Q-factor. To examine the relationship between Q-factor and grating depth, an RCWA software package (Diffract MOD, RSOFT Design) was used to calculate the transmission efficiency as a function of illumination angle An incident beam of λ_{r} and θ_{r} can be coupled into a resonant mode, resulting in a dip in the transmission efficiency, as measured in the far field. PC structures with three different grating depths (15 nm, 30 nm, and 100 nm) were studied. For all three PC structures, the grating period is $\Lambda = 400$ nm while the $\mathrm{TiO_2}$ thickness was selected to maintain a resonant angle of 10° at a resonant wavelength of 633 nm ($\mathrm{t_{TiO_2}} = 155$ nm, 158 nm and 185 nm).

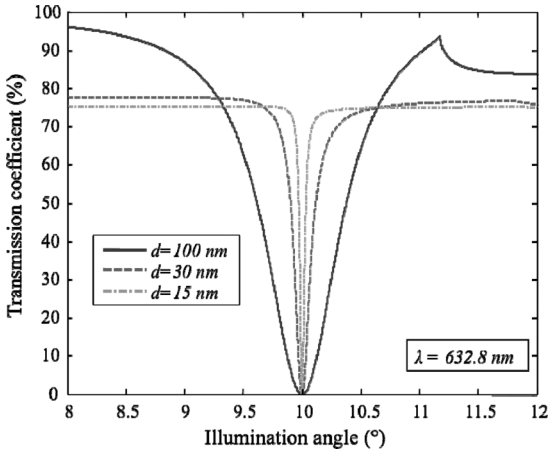

Fig. 2. Simulated transmission spectra of three different PC designs. The PC grating has depth of 15 nm, 30 nm, and 100 nm, respectively. The period of the grating is 400 nm and the TiO_2 thickness is 155 nm, 158 nm, and 185 nm, respectively, to maintain a constant angle of resonant coupling for a wavelength of $\lambda = 632.8$ nm.

The angle transmission spectra are shown in Fig. 2. As expected, using shallower grating depth increases the Q-factor. However, as the Q-factor increases, the coupling condition becomes more stringent. For example, the angle tolerance of a $d = 100$ nm grating is 0.76° but the angle acceptable range of a $d = 15$ nm grating is only 0.06°. In order to fully utilize the field enhancement capability of high Q-factor PC surfaces, the illumination must be well collimated.

B. Resonant Field Distribution in Case of Diverged Beam Excitation

Unfocused laser beams are highly collimated, but exhibit divergence that results in incident angle components with a Gaussian distribution around normal. It is particularly important to note that commercially available fluorescence laser scanners use a focused laser beam [29]–[31]. As we move towards higher Q-factors for PCEF, the angle tolerance for exciting a resonant mode decreases. Therefore, it is important to consider the beam divergence of the excitation light for optimal performance.

To quantify how beam divergence affects the enhancement factor, we developed a calculation scheme. A commercially available Rigorous Coupled Wave Analysis (RCWA) solver (RSoft DiffractMod) can only output the field distribution in a PC that is excited by a plane wave. For simulating real laser excitation conditions, we combined an analytical approach with RCWA to provide a field intensity distribution for a PC surface illuminated by any diverging beam.

We define the z axis as out of the plane of the sensor surface. The total near field amplitude distribution $\mathrm{E(x,z)}$ is averaged for a field distribution at a specific angle θ_j (j is an integer from 0 to n, where n is the total number of incident angles being simulated) weighted by the intensity of the excitation beam $\mathrm{I}(\theta_j)$. The field distribution at an individual angle, $\mathrm{E}_{\theta j}(\mathrm{x,z})$, is calculated using RCWA. The expression of $\mathrm{E(x,z)}$ is given by,

$$\mathrm{E(x,z)} = \sum_{j=0}^{n} \mathrm{I}(\theta_j)\mathrm{E}_{\theta_j}(\mathrm{x,z}). \tag{1}$$

The Spatial Intensity distribution of a Gaussian beam propagating along the z-axis is given by,

$$\mathrm{I(x,z)} = \mathrm{I_0}\left[\frac{\mathrm{w_0}}{\mathrm{w(z)}}\right]^2 \mathrm{e}^{-\left(2\mathrm{x}^2/\mathrm{w}^2(\mathrm{z})\right)}. \tag{2}$$

where $\mathrm{w_0}$ and $\mathrm{w(z)}$ represent the minimum spot size and spot size at z, respectively [32].

In order to find the intensity distribution in terms of angle, the spatial distribution function is transformed into k-space governed by $\mathrm{I(x,z)} \langle = \rangle \mathrm{I}(\theta, \mathrm{z})$. The expression of the angle dependent intensity distribution function is

$$\mathrm{I}(\theta) = \mathrm{I_0}\sqrt{\frac{\pi}{2}}\left[\frac{\mathrm{w_0}}{\mathrm{w(z)}}\right]^2 \mathrm{e}^{-(1/2)\left((\mathrm{k_0}\sin\theta)^2(\mathrm{w}^2(\mathrm{z})/8)\right)}. \tag{3}$$

After focusing by a lens with a focal length f, the angle intensity distribution is given by

$$\mathrm{I}(\theta) = \mathrm{I_0'}\mathrm{e}^{-(1/2)((\mathrm{k_0}\sin\theta)(\lambda \mathrm{f}/\pi \mathrm{L}))^2}. \tag{4}$$

where L represents the diameter of the laser beam. In the case of beam illumination at the resonant angle θ_r , (4) can be written as

$$\mathrm{I}(\theta - \theta_r) = \mathrm{I_0'}\mathrm{e}^{-(1/2)\left((1/\pi)^2\mathrm{F}^2\mathrm{k_0^2}\sin^2(\theta-\theta_r)\right)}. \tag{5}$$

where $\mathrm{F} = \mathrm{f/L}$. Substituting (5) into (1), the averaged field amplitude is given by

$$\mathrm{E(x,z)} = \sum_{j=0}^{n} \mathrm{I}(\theta_j - \theta_r)\mathrm{E}_{\theta_j}(\mathrm{x,z}). \tag{6}$$

C. Simulation of Field Enhancement Factor

Using the developed numerical methods, we evaluated the field enhancement factor for the PC structures. Since the resonant angle of the PC surfaces are designed for an incident angle of $\theta = 10°$, the RCWA was used to calculate field distributions in one period of the PC for $0° < \theta < 20°$ with increments of 0.01°. The illumination intensity at a particular angle (θ_j) is calculated using (5) and multiplied with the field amplitude distribution, $\mathrm{E}_{\theta j}(\mathrm{x,z})$ which was simulated using RCWA. The averaged field intensity was found by taking the square of $\mathrm{E(x,z)}$. Since the PC enhancement is a near field effect that is localized to the vicinity of sensor surface, only the field intensity within a 50 nm region above surface is counted. The ratio of the averaged field intensity as compared to the intensity on a reference glass slide is defined as the enhancement factor. Assuming a laser spot with 1 mm diameter, the divergence of the beam after focusing can be altered using a lens with different focal lengths. In our simulation, we consider the laser beam with divergence between 3.3° to 0.00033°. As shown in Fig. 3, when the excitation beam is highly diverging, the enhancement factor of a low Q-factor PC is higher than that of the high Q-factor PC. However, the high Q-factor PC exhibits an enhancement factor of 263 × if the excitation beam becomes more collimated. An excitation beam with angle of divergence beyond 0.005° can be fully coupled into the resonance. An excessively collimated beam will not result in a better enhancement factor once the coupling condition is met.

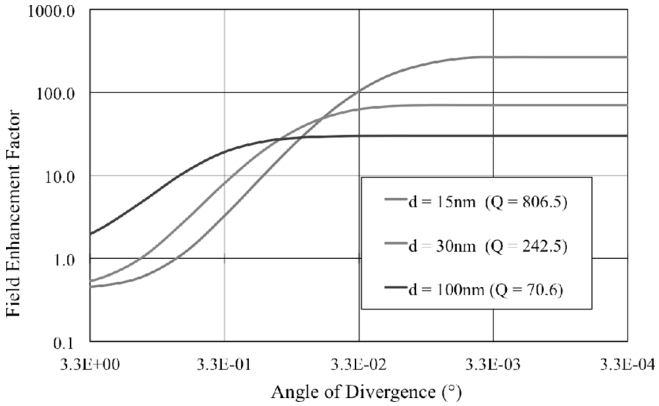

Fig. 3. Simulated local field enhancement factor in terms of angle divergence of the excitation laser beam for PC substrates with different Q-factors.

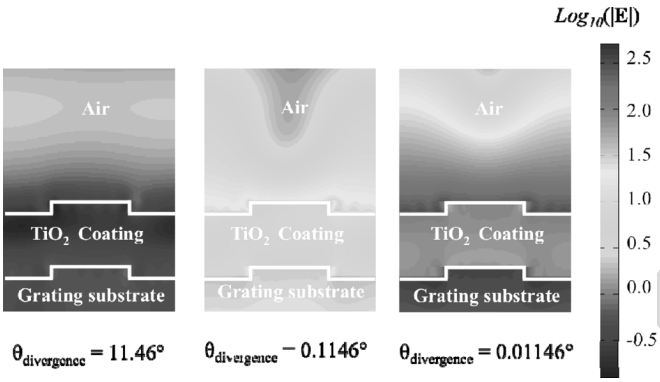

Fig. 4. Simulated local field enhancement factor in terms of angle divergence of the excitation laser beam for PC surfaces with different angle of divergence for a 15 nm depth grating.

To further illustrate the field enhancement effect, the averaged near field intensities of gratings with depth $\mathrm{d} = 15\,\mathrm{nm}$ were calculated and compared in Fig. 4 for three exemplary excitation beams with divergence of 11.46°, 0.1146°, and 0.01146°. We investigate the effect of variations in excitation beam divergence to near field strength. In Fig. 4, the field distribution in a single period of the PC structure is plotted at the resonant wavelength. The white contour highlights the surface of the grating substrate and the top of the PC surface. Fig. 4(a) demonstrates the field intensity distribution at laser beam divergence of 11.46°. Compared to the mode profile given in Fig. 4(a), the near field shown in Fig. 4(b) is ~ 60 times stronger when the excitation beam is less divergent (0.1146°). For the case of least divergence shown in Fig. 4(c), the field intensity is highest (~ 507 times higher than the most divergent case). This example illustrates that using a highly collimated excitation source is critical to achieving the greatest enhanced near field.

III. PC Enhanced Fluorescence Instrumentation

Two different types of fluorescence detection systems were studied for PCEF: a commercially available microarray laser scanner and a modified fluorescence microscope that is specifically designed for PCEF. The apparatus of the microarray laser scanner (LS Reloaded, Tecan Inc.) is shown in Fig. 5(a). This system uses a focused laser beam (beam divergence $\sim 2.5°$) as the excitation source and a photomultiplier tube (PMT) as

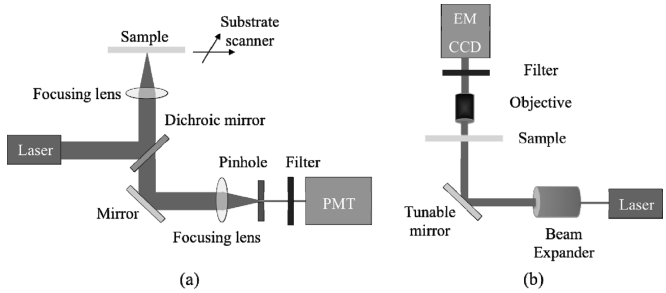

Fig. 5. (a) Schematic diagram of optical setup of the confocal laser scanner and (b) schematic drawing of PC enhanced fluorescence microscope. (a) Microarray laser scanner. (b) PC enhanced fluorescence microscope.

the fluorescence signal detector. In order to form an image, the substrate is scanned and the fluorescence signal intensity for each pixel is acquired. The apparatus of the custom-built fluorescent detection system, which is referred as the PC Enhanced Fluorescence Microscope (PCEFM), is shown in Fig. 5(b). In the PCEFM system, the fluorescent sample is imaged by an electron multiplying charge coupled device (EMCCD; Hammamatsu Inc.) via a $4\times$ microscope objective (numerical aperture $\mathrm{N.A.} = 0.1$). Unlike the confocal laser scanner, the PCEFM works in the imaging mode, which significantly improves the measurement throughput. For both systems, a HeNe laser ($\lambda = 632.8\,\mathrm{nm}$) is used as an excitation light source, and a bandpass filter is placed in front of the detectors to reject excitation laser light.

The microarray laser scanner uses a lens with a high numerical aperture (N.A.) to focus the laser beam on to the sample and collects the fluorescence signal resulting from this excitation. Due to the focusing effect, the illumination laser beam angle spans from 0° to 30°. As a result, only a small portion of the excitation energy can be coupled into the resonant mode of the PC surface, thus compromising the enhancement performance of the PC. For the PC surface with $\mathrm{Q} \sim 300$, the coupling efficiency is less than 20%. As discussed above, in order to take full advantage of a PC and accomplish high enhancement of the fluorescence signal, it is critical to achieve a good coupling efficiency between the excitation laser beam and the PC surface. The PCEFM setup is designed specifically to achieve this and utilizes collimated illumination for this purpose. As shown in Fig. 5(b), the output of the HeNe laser is expanded to produce a beam with diameter of 20 mm and divergence of 0.037° using a beam expander. In order to accurately control the angle of incidence, the PCEFM system utilizes a high precision angle tuning gimbal-mounted mirror which is itself is mounted on a motorized linear stage that moves as the mirror rotates. The movement of this linear stage compensates the beam shift due to incident angle variation and thereby ensures a fixed illumination area. The angle tuning resolution of this configuration is 0.005°, resulting in the capability for testing PC devices with angle bandwidth as narrow as 0.01°. A coupling efficiency of 98% has been achieved using this system with a PC surface with angle bandwidth of 0.3°.

IV. Coupling of PC Sensor and Excitation Light

The PC sensor used in this paper was fabricated using nanoimprint lithography (NIL) [33], [34]. The detailed fabrication

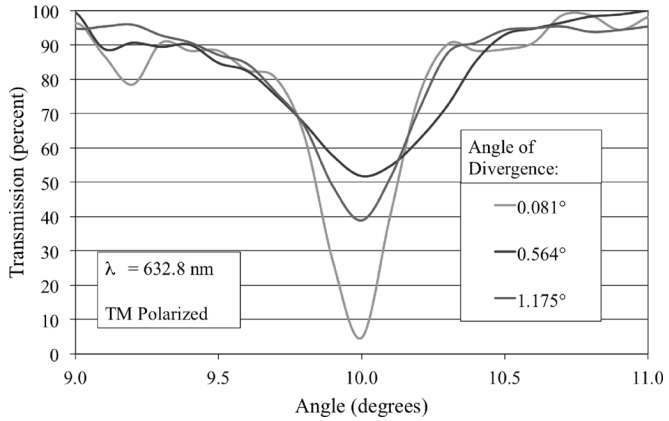

Fig. 6. Transmission spectrum of a PC enhancement substrate where the resonant angle is around 10°. The illumination spot is has divergence of 1.175°, 0.564°, and 0.081°.

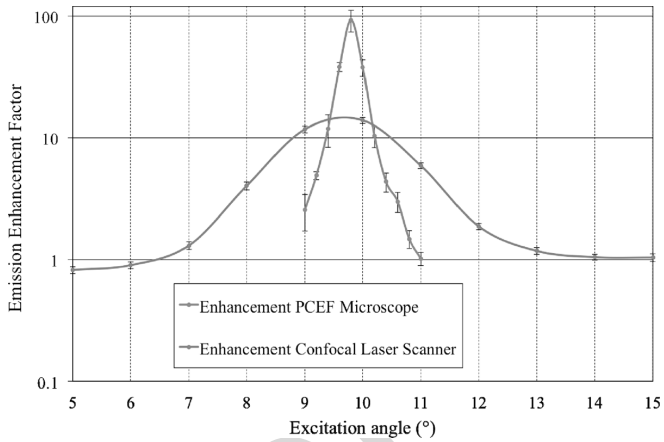

Fig. 7. Comparison of the fluorescence intensity as a function of excitation angle measured using the PCEF microscope and the Confocal Laser Scanner.

procedure has been fully described in a previous publication [35]. The fabricated PC structure has a period of $\Lambda = 400\ \mathrm{nm}$, duty cycle of 50%, and grating depth of $\mathrm{d} = 40\ \mathrm{nm}$. As a high index layer, 130 nm of $\mathrm{TiO_2}$ was coated by RF-sputtering. Illuminated by a HeNe laser at $\lambda = 632.8\ \mathrm{nm}$, this PC exhibits resonance at an angle of $\theta = 10°$. The coupling between the PC resonant mode and laser beam with different degrees of divergence was investigated. The enhancement capability of the PC was compared between the confocal laser scanner and the PCEFM.

A. Transmission Spectrum

In order to show the effect of laser beam divergence on the coupling between the PC and excitation light, we measured the transmission spectrum using focused and non-focused beams as illumination sources. To measure the transmission spectrum in terms of angle, the sample was illuminated by a HeNe laser and the transmitted light power was monitored by a silicon photodetector while the angle of incidence was scanned around the resonant angle (9° to 11.5°). Low transmission (high reflection) efficiency indicates good coupling of incident light into the resonant mode of the PC. By using lenses of different focal lengths, we varied the divergence of the incident laser beam. Without a focusing lens, the divergence angle is 0.081°, using lenses with focal lengths of 125 mm and 60 mm, the beam divergences are 0.564° and 1.175°, respectively. As shown in Fig. 6, the measured transmission spectra were compared for the collimated and non-collimated illumination. Using a collimated laser beam, the transmission efficiency was 5% at resonant angle with angle full-width half maximum of 0.37°. The transmission efficiency increases to 39% and 51% when the laser beam was focused by lenses with 125 mm and 60 mm focal lengths, respectively. Due to the broadening of incidence angle, a lower percentage of excitation energy is coupled into resonance, and transmission efficiency becomes higher. With regard to PC enhanced fluorescence, the diverged beam results in only a portion of the excitation energy being amplified by the PC resonance, which diminishes the fluorescence enhancement capability of the PC sensor.

B. Enhanced Fluorescence Intensity

Having established a clear relationship between degree of collimation of incident light and coupling efficiency with a PC, we performed fluorescence measurements to experimentally correlate the influence of degree of collimation of incident light with the extent of fluorescence enhancement. We used the microarray laser scanner and the PCEFM discussed in Section III, to represent cases for focused and collimated light. The signal enhancement factor for the on-resonance case with respect to the off-resonance case was measured over a range of angles around the resonance angle. This is shown in Fig. 7.

The collimated light gave a signal enhancement factor almost $7\times$ higher than the case for the focused light. This can be easily explained as a direct consequence of the higher magnitude of surface localized electric field intensity that interacts with fluorophores immobilized on the surface of the PC.

Another interesting observation was that the signal enhancement is much more sensitive to the proximity to the resonance angle for collimated excitation ($\mathrm{FWHM}_\theta < 0.4°$) when judged against focused excitation (peak $\mathrm{FWHM}_\theta > 1.5°$). This can be explained as a consequence of the sensitivity of the coupling efficiency of the PC to change in excitation angle for collimated light. Thus, for the PCEFM a small deviation from the resonance condition will result in a large drop in the surface localized electric field intensity, ultimately leading to lower enhancement in fluorescence intensity. For the case of focused light, since the incident beam consists of a spread of angles, over a fairly large range there will be some amount of light that will always be present in the resonant angle range. Thus, even though the coupling will never be as efficient and the electric field intensities will never reach high values, the fluorescence enhancement will have a much greater angle tolerance. Thus the degree of collimation of the excitation light (which influences the coupling efficiency of the PC as described in the previous section) is the ultimate determining factor for the degree of enhancement. The sensitivity of the degree of enhancement to the proximity to the resonance angle has far-reaching implications for performing multiplexed assays on a PC surface.

For relating our enhancement factors on the PC to a glass slide we performed a study to analyze the total enhancement of the PC on-resonance when compared to unpatterned glass. Fig. 8 shows a bar graph plot for the signal enhancement as measured on the PCEFM and the confocal laser scanner. The plot shows a very high signal enhancement for the on-resonance case compared to the off-resonance case ($169\times$ for PCEFM, and $15\times$

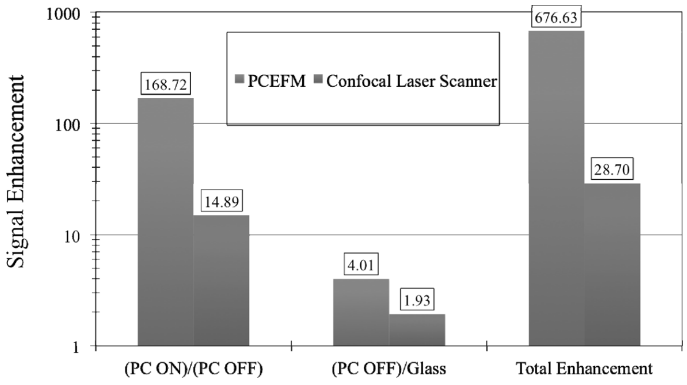

Fig. 8. Comparison of the fluorescence enhancement using the PCEF microscope and the Confocal Laser Scanner. The fluorescence signal enhancement for the PC on resonance compared to the off resonance case is attributed to the "enhanced excitation" property of the PC. The fluorescence signal enhancement for the PC off resonance compared to unpatterned glass is attributed to the "enhanced extraction" property of the PC. The total enhancement is the ratio of the fluorescence signal for the PC on resonance to the unpatterned glass.

for the laser scanner) which is due to the enhanced excitation effect. The off-resonance case for the PC also has a higher signal as compared to a glass slide ($\sim 4\times$ for the PCEFM and $\sim 2\times$ for the laser scanner). This is a result of the PC enhanced extraction effect [14]. In this case, emitted photons, which would ordinarily exit the surface distributed uniformly in all directions, are spatially biased away from the PC surface at an (approximately) normal angle, so they may be gathered more efficiently by the detection optics.

The combination of the two enhancement effects provides a net signal enhancement (compared to unpatterned glass) of $\sim 677\times$ using the PCEFM and $\sim 29\times$ using the laser scanner.

C. Angle-Scanned Image Optimization

Having established the superior performance of a PC under collimated conditions and the promise of high enhancement offered by the PCEFM, it is necessary to provide a uniform enhancement effect over substantial surface areas, such as those used for protein microarrays or DNA microarrays that are comprised of hundreds or thousands of capture spots. Because the enhancement factor is highly sensitive to the angle of incidence for a collimated beam (Fig. 7), small variations in the PC surface resonant coupling angle caused by nonuniformities in the PC structure (for example, the TiO_2 layer thickness) and the density of surface functionalization layers will result in substantial variations in fluorescent intensity if a fixed incident angle is used to scan the entire device. This problem is further complicated by the variable density of immobilized capture molecules, such as DNA or antibodies that are deposited as arrays of spots on the PC surface. Capture molecules are typically deposited with high density, and therefore result in a substantially lower PC coupling angle compared to the regions of the surface between capture spots. There is thus no single incident angle that can be used to optimally couple a laser to every region of a PC surface.

In order retain the benefits of signal enhancement while still performing fast high throughput measurements; we developed a methodology to account for the variation in the resonant coupling angle across the device. Rather than gathering fluorescent

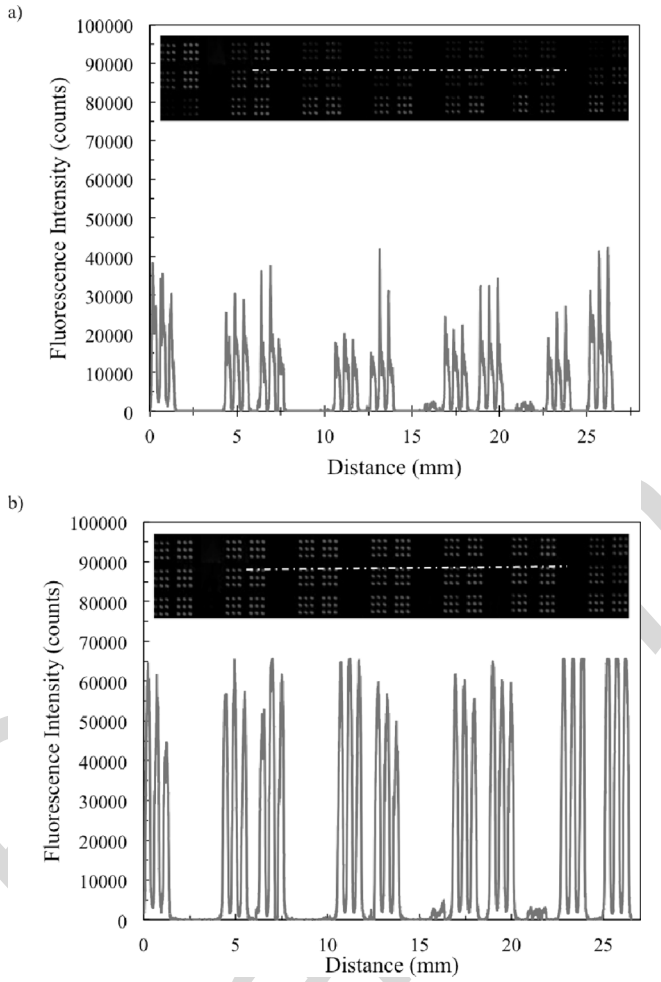

Fig. 9. Intensity profile as a function of distance for a line of fluorescent image pixels profiling spots of Alexa-647 conjugated PPL for the PC: (a) using a fixed excitation angle at 10° and (b) the fluorescence intensity is scanned at 11 angles near the resonance angle. The scanned images are shown in insets.

output images with the PCEFM using a single incident angle, we capture a sequence of fluorescence images over a range of angles that always includes the resonance angle. Software is used to compare the images taken at each angle, and to select the maximum intensity of every pixel over the scanning range. Because the maximum intensity for any pixel will always be generated when the incident angle matches the optimal resonant condition, a new image can constructed using the maximum intensity angle for each pixel.

To demonstrate the angle-scanning method, a 3×3 array of Poly(Lys, Phe) conjugated with Alexa-647 (Invitrogen) was spotted at a concentration of 9.9 $\mu g/ml$ onto the 1×3 in^2 PC surface by a piezoelectric dispenser (Piezorray, Perkin Elmer) with a center-to-center separation of 500 μm and a spot radius of ~ 200 μm. Prior to spotting, the PC surface was pre-cleaned with O_2 plasma for 3 min. and then cleaned by sonication in acetone, isopropanol and deionized (DI) water and followed by drying under a nitrogen stream. After spotting, the PC was incubated for 24 hours in a sealed container. The spot densities were selected so as to give an approximate shift of $-0.2°$ in the PC coupling condition.

Selecting a single incident angle of $\theta = 10°$, the PCEFM gathered the image shown in Fig. 9(a). Using a $4\times$ microscope

objective, a single fluorescent image has a field of view of $\sim 2 \times 2\ \mathrm{mm}^2$. An automated motion stage enables capture of fluorescent images from adjacent regions, and concatenation of images results in a fluorescent image of the entire slide, using a total scanning time of 24 seconds. Nominally, each spot in the array is identical, but the fluorescent intensity shows the effects of nonoptimal laser coupling to the PC resonance in several regions of the chip, resulting in a coefficient of variability of $\mathrm{CV} = 51\%$ for the on-spot intensity.

Fig. 9(b) is a fluorescence image of the same slide as Fig. 9(a) with the image constructed by the new methodology. For each imaged region, a sequence of fluorescence intensity images is gathered from $9.5^\circ < \theta < 10.5^\circ$ in 0.1° increments, for a total of 11 images per frame. By gathering the additional images, the scanning time for the entire $1 \times 3\ \mathrm{in}^2$ area increased to 48 sec. The maximum-pixel selection and composite image-processing algorithm runs in 60 sec. As a result of the new method, the spot CV is reduced to 17.9%. This level of spot-to-spot variability is consistent with what is typically obtained for fluorescent images of spot intensities on glass surfaces (data not shown), and therefore represents variability due to the spots themselves, rather than variability in the detection method. Using the angle scanning approach, we observe a consistently high enhancement factor across the entire PC area.

V. Conclusion

We have reported on the study of PC enhanced fluorescence illuminated with laser beams with different degrees of divergence. By use of an imaging system that enables angle-tunable collimated illumination of the PC surface, we have established improved performance for PC when subjected to collimated excitation as compared to focused excitation in a confocal laser scanner, demonstrating raw signal enhancement of 677 $\times$. The signal enhancement is accompanied by an extreme sensitivity to the angle of excitation. This results in a problem of variability when attempting to utilize the PCEFM for high throughput measurements, such as those used in DNA microarrays or protein microarrays. In order to address this issue, an angle-scanning method was developed that allows optimal coupling to every pixel in a PC-based fluorescent image, and thus achieves a uniformly high enhancement factor over large surface areas.

References

[1] J. W. Lichtman and J.-A. Conchello, "Fluorescence microscopy," *Nature Methods*, vol. 2, no. 12, p. 910(10), 2005.

[2] J. Stenken, "Introduction to fluorescence sensing," *J. Amer. Chem. Soc.*, vol. 131, no. 30, p. 10791, 2009.

[3] W. Budach *et al.*, "Generation of transducers for fluorescence-based microarrays with enhanced sensitivity and their application for gene expression profiling," *Anal. Chem.*, vol. 75, pp. 2571–2577, 2003.

[4] H. Jin and R. C. Zangar, "Protein modifications as potential biomarkers in breast cancer," *Biomarker Insights*, vol. 2009, no. 1761, p. 191, 2009.

[5] P. C. Mathias, H.-Y. Wu, and B. T. Cunningham, "Employing two distinct photonic crystal resonances to improve fluorescence enhancement," *Appl. Phys. Lett.*, vol. 95, no. 2, p. 021111, 2009.

[6] N. Ganesh *et al.*, "Leaky-mode assisted fluorescence extraction: Application to fluorescence enhancement biosensors," *Opts. Exp.*, vol. 16, no. 26, pp. 21626–21640, 2008.

[7] I. D. Block *et al.*, "A detection instrument for enhanced-fluorescence and label-free imaging on photonic crystal surfaces," *Opt. Exp.*, vol. 17, no. 15, pp. 13222–13235, 2009.

[8] H. Y. Wu *et al.*, "Magnification of photonic crystal fluorescence enhancement via TM resonance excitation and TE resonance extraction on a dielectric nanorod surface," *Nanotechnology*, vol. 21, no. 12, pp. 125–203, Mar. 2010.

[9] P. C. Mathias, H.-Y. Wu, and B. T. Cunningham, "Employing two distinct photonic crystal resonances for improved fluorescence enhancement," *Appl. Phys. Lett.*, vol. 95, no. 2, p. 021111, 2009.

[10] P. C. Mathias, N. Ganesh, and B. T. Cunningham, "Application of photonic crystal enhanced fluorescence to a cytokine immunoassay," *Anal. Chem.*, vol. 80, no. 23, pp. 9013–9020, 2008.

[11] B. T. Cunningham *et al.*, "A plastic colorimetric resonant optical biosensor for multiparallel detection of label-free biochemical interactions," *Sens. Actuators B*, vol. 85, no. 3, pp. 219–226, 2002.

[12] I. D. Block, L. L. Chan, and B. T. Cunningham, "Photonic crystal optical biosensor incorporating structured low-index porous dielectric," *Sens. Actuators B*, vol. 120, no. 1, pp. 187–193, Dec. 2006.

[13] B. T. Cunningham *et al.*, "Label-free assays on the BIND system," *J. Biomolecular Screening*, vol. 9, pp. 481–490, 2004.

[14] B. T. Cunningham and L. L. Laing, "Label-free detection of biomolecular interactions: Applications in proteomics and drug discovery," *Expert Reviews in Proteomics*, vol. 3, no. 3, pp. 271–281, 2006.

[15] L. Chan *et al.*, "A label-free photonic crystal biosensor imaging method for detection of cancer cell cytotoxicity and proliferation," *Apoptosis*, vol. 12, no. 6, pp. 1061–1068, 2007.

[16] L. L. Chan *et al.*, "Label-free imaging of cancer cells using photonic crystal biosensors and application to cytotoxicity screening of a natural compound library," *Sens. Actuators B*, vol. 132, pp. 418–425, 2008.

[17] L. L. Chan *et al.*, "A self-referencing method for microplate label-free photonic crystal biosensors," *IEEE Sensors J.*, vol. 6, no. 6, pp. 1551–1556, Dec. 2006.

[18] L. L. Chan *et al.*, "General method for discovering inhibitors of protein-DNA interactions using photonic crystal biosensors," *ACS Chem. Biol.*, vol. 3, no. 7, pp. 437–448, 2008.

[19] P. Li *et al.*, "A new method for label-free imaging of biomolecular interactions," *Sens. Actuators B, Chem.*, vol. 99, pp. 6–13, 2004.

[20] A. Hessel and A. A. Oliner, "A new theory of Wood's anomalies on optical gratings," *Appl. Opt.*, vol. 4, no. 10, pp. 1275–1297, 1965.

[21] E. Popov, L. Mashev, and D. Maystre, "Theoretical-study of the anomalies of coated dielectric gratings," *Optica Acta*, vol. 33, no. 5, pp. 607–619, May 1986.

[22] L. Mashev and E. Popov, "Diffraction efficiency anomalies of multicoated dielectric gratings," *Opt. Commun.*, vol. 51, no. 3, pp. 131–136, 1984.

[23] L. Mashev and E. Popov, "Zero order anomaly of dielectric coated gratings," *Opt. Commun.*, vol. 55, no. 6, pp. 377–380, 1985.

[24] N. Ganesh *et al.*, "Distance dependence of fluorescence enhancement from photonic crystal surfaces," *J. Appl. Phys.*, vol. 103, p. 083104, 2008.

[25] P. Kramper *et al.*, "Direct spectroscopy of a deep two-dimensional photonic crystal microresonator," *Phys. Rev. B*, vol. 64, no. 23, p. 233102, 2001.

[26] C. J. Barrelet *et al.*, "Hybrid single-nanowire photonic crystal and microresonator structures," *Nano Lett.*, vol. 6, no. 1, pp. 11–15, Jan. 2006.

[27] P. C. Mathias *et al.*, "Graded wavelength one-dimensional photonic crystal reveals spectral characteristics of enhanced fluorescence," *J. Appl. Phys.*, vol. 103, p. 094320, 2008.

[28] I. D. Block *et al.*, "A sensitivity model for predicting photonic cyrstal biosensor performance," *IEEE Sensors J.*, vol. 8, no. 3, pp. 274–280, Mar. 2008.

[29] K. J. Halbhuber and K. Konig, "Modern laser scanning microscopy in biology, biotechnology and medicine," *Ann. Anatomy-Anatomischer Anzeiger*, vol. 185, no. 1, pp. 1–20, Jan. 2003.

[30] W. B. Amos and J. G. White, "How the confocal laser scanning microscope entered biological research," *Biol. Cell*, vol. 95, no. 6, pp. 335–342, 2003.

[31] S. Paddock, "Over the rainbow: 25 Years of confocal imaging," *BioTechniques*, vol. 44, no. 5, pp. 643–648, 2008.

[32] B. E. A. Saleh and M. C. Teich, *Fundamentals of Photonics*, 1st ed. New York: Wiley, 1991, pp. 80–107.

[33] S. Y. Chou, P. R. Krauss, and P. J. Renstrom, "Imprint of sub-25 nm vias and trenches in polymers," *Appl. Phys. Lett.*, vol. 67, no. 21, pp. 3114–3116, 1995.

[34] S. Y. Chou, P. R. Krauss, and P. J. Renstrom, "Imprint lithography with 25-nanometer resolution," *Science*, vol. 272, no. 5258, pp. 85–87, Apr. 1996.

[35] A. Pokhriyal *et al.*, "Photonic crystal enhanced fluorescence using a quartz substrate to reduce limits of detection," *Opt. Exp.*, vol. 18, no. 24, pp. 24793–24808, 2010.

Vikram Chaudhery received the B.S. and M.S. degrees in electrical and computer engineering from the University of Illinois at Urbana–Champaign, Urbana, in 2009 and 2011, respectively. Currently, he is working towards the Ph.D. degree as a Graduate Research Assistant under the direction of Prof. Brian T. Cunningham at the University of Illinois at Urbana–Champaign.

His research focuses on the design, characterization and optimization of novel detection and imaging instrumentation for photonic crystal biosensors and its application in life sciences.

Meng Lu received the B.S. degree in electrical and computer engineering from University of Science and Technology of China, Beijing, in 2002, and the M.S. and Ph.D. degrees in electrical and computer engineering from the University of Illinois at Urbana–Champaign, Urbana, in 2004 and 2008, respectively.

His research at the University of Illinois at Urbana–Champaign under the direction of Prof. Brian T. Cunningham focused on the development of optical sensor systems. He is currently with SRU Biosystems, Woburn, MA, working on optical biosensors.

Anusha Pokhriyal received the M.S. degree in physics from Worcester Polytechnic Institute, Worcester, MA, in 2008. She is currently working towards the Ph.D. degree as a Graduate Research Assistant under the direction of Prof. Brian T. Cunningham at the University of Illinois at Urbana–Champaign, Urbana.

Her research focuses on the design and characterization of optical biosensors and device fabrication processes.

Stephen C. Schulz, photograph and biography not available at the time of publication.

Brian Cunningham received the B.S., M.S., and Ph.D. degrees in electrical and computer engineering from the University of Illinois at Urbana–Champaign, Urbana. His thesis research was in the field of optoelectronics and compound semiconductor material science, where he contributed to the development of crystal growth techniques that are now widely used for manufacturing solid state lasers, and high-frequency amplifiers for wireless communication.

He is a Professor in the Department of Electrical and Computer Engineering and the Department of Bioengineering at the University of Illinois at Urbana–Champaign, where he has been a faculty member since 2004. His group focuses on the development of nanophotonic surfaces, plastic-based nanofabrication methods, and novel instrumentation approaches for biodetection with applications in pharmaceutical screening, life science research, environmental monitoring, disease diagnostics, and point-of-care patient testing. At the University of Illinois at Urbana–Champaign, he serves as the Director of the Bioengineering Graduate Program and Director of the NSF Center for Agricultural, Biomedical, and Pharmaceutical Nanotechnology (CABPN). He is a founder and the Chief Technical Officer of SRU Biosystems, Woburn, MA, a life science tools company that provides high sensitivity plastic-based optical biosensors, instrumentation, and software to the pharmaceutical, academic research, genomics, and proteomics communities. Prior to founding SRU Biosystems in June 2000, he was the Manager of Biomedical Technology at Draper Laboratory, Cambridge, MA, where he directed R&D projects aimed at utilizing defense-related technical capabilities for medical applications. In addition, he served as Group Leader for MEMS Sensors at Draper Laboratory, where he directed a group performing applied research on microfabricated inertial sensors, acoustic sensors, optical switches, microfluidics, tissue engineering, and biosensors. Concurrently, he was an Associate Director of the Center for Innovative Minimally Invasive Therapy (CIMIT), a Boston-area medical technology consortium, where he led the Advanced Technology Team on Microsensors. Before working at Draper Laboratory, he spent five years at the Raytheon Electronic Systems Division developing advanced infrared imaging array technology for defense and commercial applications.

Prof. Cunningham was recognized with the IEEE Sensors Council 2010 Technical Achievement Award for the invention, development, and commercialization of biosensors utilizing photonic crystals.